The self-consistent response of linear microinstabilities to profile evolution

A. Bokshi[1], J. W. Connor[2], D. Dickinson[1], C. M. Roach[2] and H. R. Wilson[1]

[1] *York Plasma Institute, Dept. of Physics, University of York, Heslington, York YO10 5DD, UK*

[2] *EUROfusion CCFE, Culham Science Centre, Abingdon, Oxon OX14 3DB, UK*

Toroidal drift instabilities are characterised by short wavelengths perpendicular to the magnetic field lines and extended structures along them. They are strongly localised in the vicinity of rational flux surfaces (that minimises field-line bending), with the flux surface spacing given by $\Delta = 1/nq'$ (n is the toroidal mode number and q' is the radial derivative of the safety factor profile). For high-n instabilities thought to be responsible for micro-turbulence $\Delta \ll L_{eq}$, with L_{eq} characterising the scale-length over which equilibrium profiles vary. The *ballooning formalism* exploits this approximate invariance of rational surfaces, and expands in the small parameter Δ/L_{eq} to reduce a system describing a 2D perturbation (in x and θ) to two uncoupled 1D equations (in the extended field-aligned coordinate η (related to θ) and the radial coordinate x). The lowest order eigenvalue problem is one in η: the formalism predicts the mode structure along η and the *local* eigenvalue $\Omega_0(x,\eta_0) = \omega_0(x,\eta_0) + i\gamma_0(x,\eta_0)$. At this order η_0 is a free parameter and is typically chosen to maximise the instability growth-rate. The next order problem is in x: the theory uses the radial variation in $\Omega_0(x,\eta_0)$ to construct the global mode structure and true eigenvalue $\Omega = \omega + i\gamma$. The higher-order theory *predicts* η_0, which is the poloidal location where the instability peaks.

This formalism can be applied to all classes of toroidal microinstabilities (e.g. ITG, MTM, KBM) and in doing so predicts two distinct solutions for each class [1, 2, 3, 4]: the *Isolated Mode* (IM) and the *General Mode* (GM). The IM is a strongly unstable mode but exists under special conditions requiring the stationary points in $\omega_0(x)$ and $\gamma_0(x)$ to be co-located. The mode typically peaks around the outboard midplane. The GM is relatively benign but occurs more generally, and is seen to peak away from the outboard midplane (illustrated in Fig. 1). The presence of a radially varying flow-shear can Doppler-shift the mode frequency, making the IM transiently accessible [3]. Here we explore the dynamics of this transition using a global fluid-ITG model and present initial results from a more self-consistent treatment, accounting for the feedback of the mode on the flow.

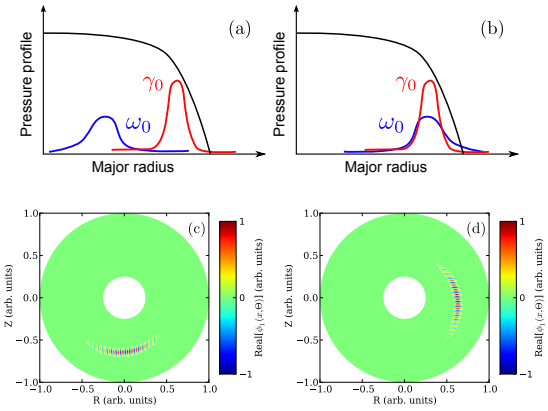

Fig. 1: *In the pedestal, the GM (a) is more likely to be present, but the IM (b) can be transiently accessed. Plots (c)-(d) show the mode structures of the GM and IM, computed using a fluid-ITG code [6].*

These results pave the way for more accurate nonlinear simulations to understand small-ELM regimes and intrinsic rotation in tokamak plasmas.

A simple linear electrostatic fluid-ITG model [5] is used to capture the essential features of toroidicity and profiles generic to all toroidal microinstabilities:

$$\left[\rho_s^2\frac{\partial^2}{\partial x^2}-k_\theta^2\rho_s^2-\frac{\sigma^2}{\Omega^2}\left(\frac{\partial}{\partial\theta}+inq\right)^2-\frac{2\varepsilon_n}{\Omega}\left(\cos\theta+\mathrm{i}\frac{\sin\theta}{k_\theta}\frac{\partial}{\partial x}\right)-\frac{\Omega-1}{\Omega+\eta_s}\right]\tilde{\phi}(x,\theta)=0. \quad (1)$$

Here $\varepsilon_n = L_n/R$ and $\sigma = \varepsilon_n/(qk_\theta\rho_s)$. We consider toroidal flow-shear Ω'_ϕ as dominant and Doppler-shift the (real part of) complex mode frequency $\Omega \to \Omega + n\Omega'_\phi x$. The perturbed potential is Fourier decomposed into poloidal harmonics $\tilde{\phi} = \sum_m \phi_m(x)\exp(-im\theta)$ and subsequently solved as an initial-value problem through a transform $\Omega \to -i\partial/\partial t$. The details of the model, its numerical implementation, equilibrium parameters and benchmarks are described in ref. [6].

We start with an eigenmode sitting at the bottom of the poloidal cross-section for a negative flow shearing-rate $\gamma_E = \Omega'_\phi/q'$ (Fig. 1(c)) and ramp it through the *critical* value needed to access the IM (in this case $\gamma_{E,\mathrm{IM}} = 0$; Fig. 2(c)). As the shear is increased further, the mode rotates to the top and, after performing several rapid poloidal precessions for $\gamma_E > \gamma_{E,\mathrm{GM}}$ (Fig. 3), settles down as a GM. We know the instability retains its eigenmode identity since all individual Fourier harmonics grow at the same rate (Fig. 2(a)). We next perform the scan in the limit $\mathrm{d}\gamma_E/\mathrm{d}t \to \infty$, to which several interesting features emerge: (1) the instability loses its eigenmode identity (as evident from the different growth-rates associated with the poloidal harmonics in Fig. 2(b)) but retains the coherent 'finger-like' structure as it gets convected poloidally; (2) the maximum growth-rate closely approaches γ_{IM}; and (3) this maximum occurs after the mode has rotated past the outboard-midplane.

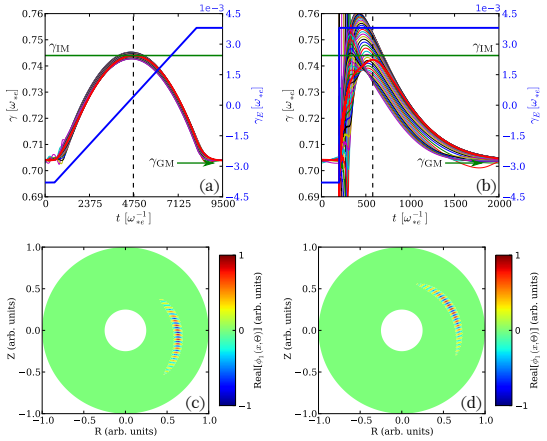

Fig. 2: *(a) shows the evolution of the growth-rate as the flow-shear is changed slowly and then (b) suddenly. Coloured lines track individual Fourier modes. (c)-(d) show the mode structure when the growth-rate is maximum. For* $\omega_{*e} = 10^6$ *Hz, 1000 units on time axis* $\sim$ *1 ms.*

This mechanism provides a new model for small-ELMs [6]. In an EPED-type model [7], we speculate that small-ELMs occur when the expanding pedestal, clamped at the marginal gradient of the GM-branch of the kinetic ballooning mode (KBM-GM), transitions to the KBM-IM as the flow-shear passes through a critical value. At this point the strongly unstable IM would drive a burst in transport, resetting the profiles and allowing the GM to re-establish. If this critical flow-

shear is not accessible, the evolving pedestal would hit the peeling-ballooning boundary and result in a Type-I ELM. For $\omega_{*e} = 10^6$ Hz, the GM-IM-GM transition is seen to occur on the $\mathcal{O}$(ms) time-scale characteristic of small-ELMs. The model provides a robust experimentally testable prediction: density/potential/magnetic fluctuations, measured inside the pedestal over a wide poloidal angle, and temporally resolved between successive small-ELM bursts, would indicate fluctuations that shift poloidally at the time of ELM onset.

Another interesting feature is the presence of Floquet Modes (FM) [8] as the GM tries to establish. For any $|\gamma_E| > \gamma_{E,\mathrm{GM}}$, instead of staying poloidally confined at the top/bottom in accordance with the eigenmode formalism, the mode rotates to the inboard side, makes a rapid transition to the outboard side and then slowly tracks its way to the top/bottom, spending more time at its eigenmode location with each precession, before eventually settling down as a GM (Fig. 3). The associated periodic burst in growth-rate as the mode samples the outboard side could further influence the small-ELM dynamics.

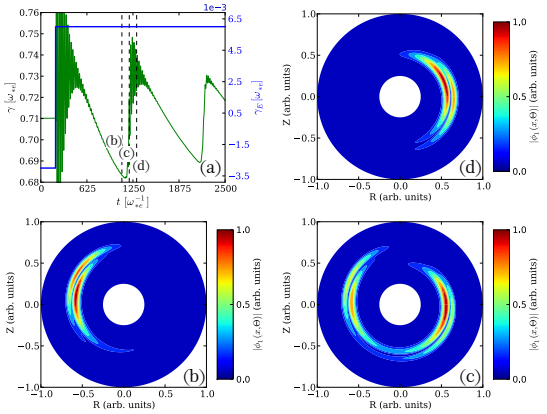

Fig. 3: *Dashed vertical lines in (a) correspond to the potential plots (b)-(d), evolving chronologically in the anti-clockwise direction.*

An important piece of physics to consider is the effect the mode structure would have on the flow through, for example, Reynolds stresses [9]. This can be incorporated into our numerical model through a flow-diffusion equation

$$\frac{\partial \langle \Omega_\phi \rangle}{\partial t} + \hat{\lambda} \frac{\partial}{\partial x} \left\langle \frac{\partial \tilde{\phi}}{\partial x} \frac{\partial \tilde{\phi}}{\partial \theta} \right\rangle = \hat{\mu} \frac{\partial \langle \Omega_\phi \rangle}{\partial^2 x} \,. \tag{2}$$

Here $\langle \ldots \rangle$ indicates a poloidal average, $\hat{\mu}$ is the viscosity and $\hat{\lambda}$ is related to the saturated mode amplitude. Since our model for $\tilde{\phi}$ (eqn. 1) is linear, $\hat{\lambda}$ is indeterminate and is taken to be such that the self-generated flow is comparable to the imposed/external flow. The steady-state solution to eqn. 2 is only dependent on the ratio $\hat{\lambda}/\hat{\mu}$, so the absolute value of $\hat{\mu}$ in these simulations is not important and has been chosen for faster numerical convergence.

Perturbed IM initialisation When the simulation is initiated with a linear flow profile and a consistent mode structure, slightly perturbed from the IM, the self-generated flow associated with the mode creates a stationary point, driving the system back towards the IM. The overall flow-profile is pushed downwards (not noticeable in these plots) as the flow locally peaks.

Floquet Mode initialisation The simulation is then initiated with an external flow-profile

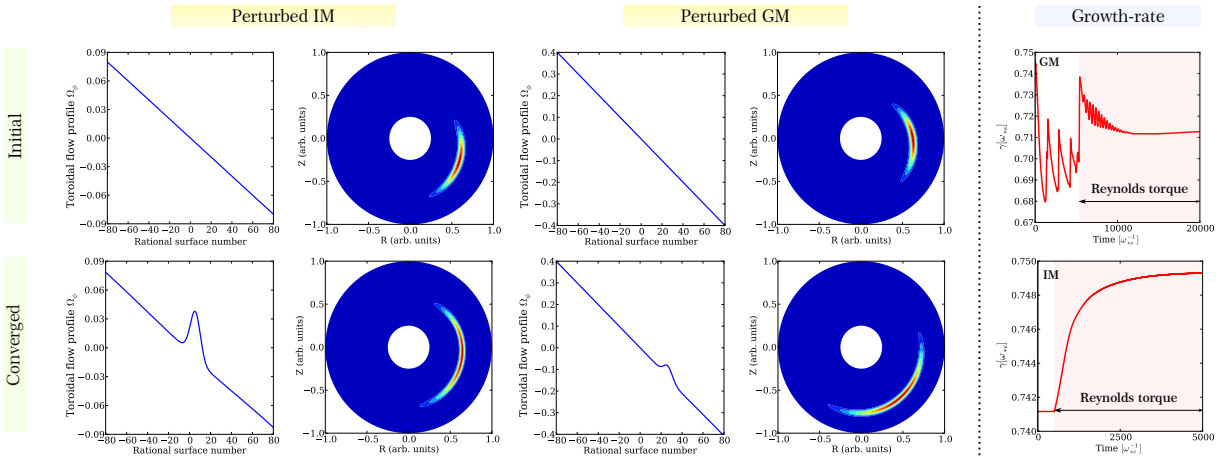

Fig. 4: *(Left of dotted line) Frames above and below show the initial and converged Ω_ϕ and $\tilde{\phi}$ for the perturbed IM and GM. (Right of dotted line) The evolution of the growth-rate for an initial GM/FM and IM with the Reynolds torque switched on at the times indicated. For these simulations $\hat{\mu} = 5.0 \times 10^{-2}$ and $\hat{\lambda} = 1.0 \times 10^{-4}$.*

such that the mode sets off performing Floquet cycles. When the intrinsic flow is switched on, depending on $\hat{\lambda}$, the peak in the flow-profile traps the mode and prevents further Floquet precessions.

The existence of IM and GM as stationary solutions would depend on the balance of the self-generated and external (e.g. equilibrium, NBI driven) torques. This can only be quantified by moving to a nonlinear model. Each global mode sitting on a resonant surface would set boundaries on the neighbouring modes; integrating across the minor radius with global boundary conditions (e.g. core NBI and SOL flows) would give the plasma rotation profile. Future work will explore the correlation between the flow associated with these linear mode structures and the saturated flows. This could potentially provide a handle on intrinsic torque profile control using shaping (for example) to modify the global mode structure.

Acknowledgements This work has been carried out within the framework of the EUROfusion Consortium and has received funding from the Euratom research and training programme 2014-18 under grant agreement No. 633053. The views and opinions expressed herein do not necessarily reflect those of the European Commission. This work was also supported by the following grants: EUROfusion Enabling Research CfP-WP15-ENR-01/CCFE-03, RCUK Energy Programme EP/I501045, EPSRC DTN EP/K504178/1, University of York's Overseas Research Scholarship and EUROfusion Fusion Researcher Fellowship WP14-FRF-CCFE/Dickinson. H. Wilson holds a Royal Society Wolfson Research Merit Award.

References

[1] J W Connor, J B Taylor and H R Wilson, *Phys. Rev. Lett.* **70** (1993) 1803
[2] J B Taylor, J W Connor and H R Wilson, *Plasma Phys. Control. Fusion* **38** (1996) 243
[3] D Dickinson, C M Roach, J M Skipp and H R Wilson, *Phys. Plasmas* **21** (2014) 010702
[4] P A Abdoul, D Dickinson, C M Roach and H R Wilson, *Plasma Phys. Control. Fusion* **57** (2015) 065004
[5] J W Connor and J B Taylor, *Phys. Fluids* **30** (1987) 3180
[6] A Bokshi, D Dickinson, C M Roach and H R Wilson, *Plasma Phys. Control. Fusion* **58** (2016) 075011
[7] P B Snyder et al, *Phys. Plasmas* **9** (2002) 2037
[8] J B Taylor and H R Wilson, *Plasma Phys. Control. Fusion* **38** (1996) 1999
[9] P H Diamond and Y B Kim, *Phys. Fluids B* **3** (1991) 1626